*Supporting Information*

# Rational Design of a P2-Type Spherical Layered Oxide Cathode for High Performance Sodium Ion Batteries

Jun Xiao,[†] Fan Zhang,[‡] Kaikai Tang,[†] Xiao Li,[†] Dandan Wang,[†] Yong Wang,*[†] Hao Liu,*[†‡] Minghong Wu*[†] and Guoxiu Wang*[‡]

[†] Joint International Laboratory on Environmental and Energy Frontier Materials, School of Environmental and Chemical Engineering, Shanghai University, Shanghai, 200444, China.
Email: yongwang@shu.edu.cn; mhwu@shu.edu.cn

[‡] Centre for Clean Energy Technology, School of Mathematical and Physical Sciences, Faculty of Science, University of Technology Sydney, Broadway, Sydney, NSW 2007, Australia.
Email: hao.liu@uts.edu.au; Guoxiu.Wang@uts.edu.au

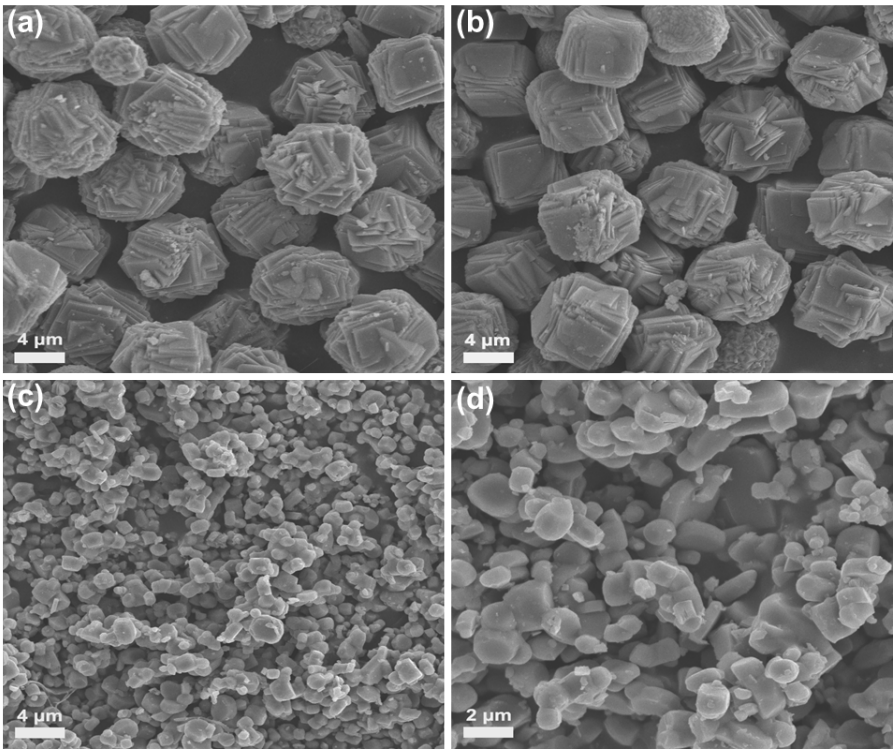


**Figure S1.** (a) SEM image of as-prepared $Mn_{0.71}Mg_{0.21}Co_{0.08}CO_3$ precursor microspheres. (b) SEM image of 400 ℃ heat treatment intermediate. (c, d) SEM images of P2-$Na_{0.66}Li_{0.18}Mn_{0.71}Mg_{0.21}$-$Co_{0.08}O_2$ (i-NaLiMMCO) synthesized by co-precipitation method.

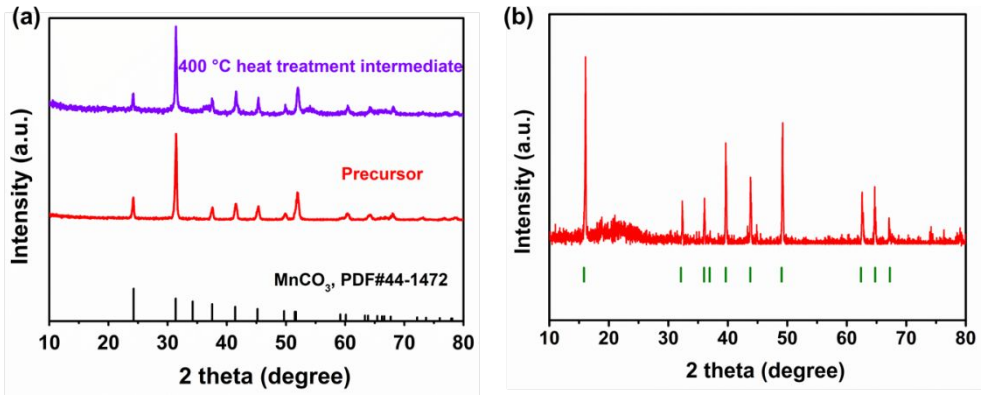


**Figure S2.** (a) XRD patterns of the $Mn_{0.71}Mg_{0.21}Co_{0.08}CO_3$ precursor microspheres (red line) and 400 ℃ heat treatment intermediate (purple line). (b) XRD pattern of P2-$Na_{0.66}Li_{0.18}Mn_{0.71}Mg_{0.21}Co_{0.08}O_2$ (i-NaLiMMCO) synthesized by co-precipitation method.

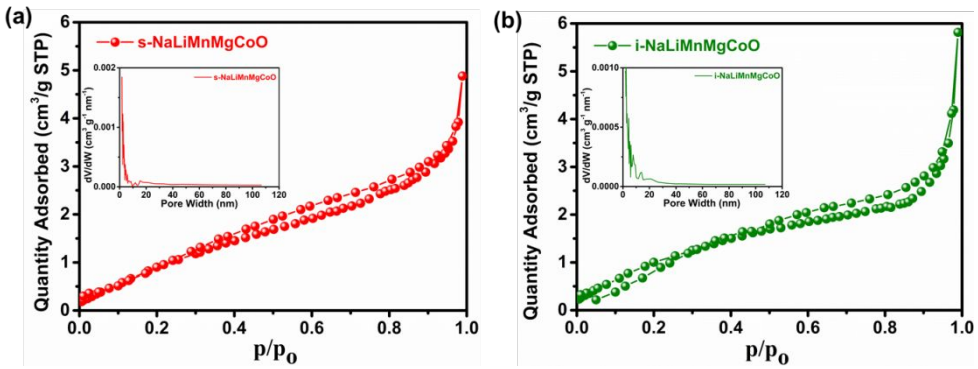


**Figure S3.** (a) $N_2$ adsorption/desorption isotherm of s-NaLiMMCO**.** (b) $N_2$ adsorption/desorption isotherm of i-NaLiMMCO.

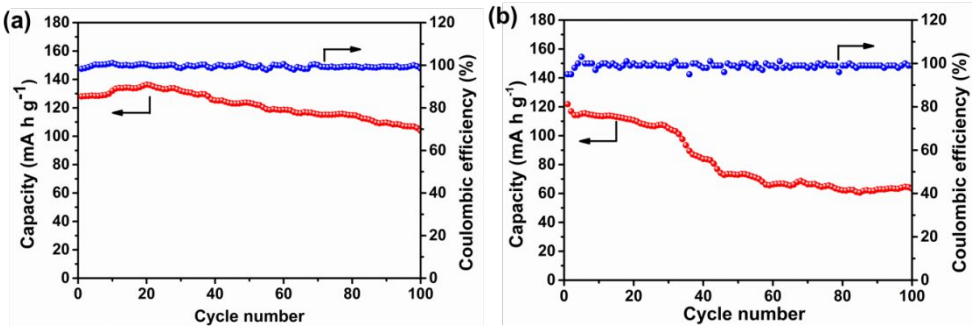


**Figure S4.** (a) The cycle performance of the s-NaLiMMCO at a rate of 100 mA $g^{-1}$. (b) The cycle performance of the i-NaLiMMCO at a rate of 100 mA $g^{-1}$.

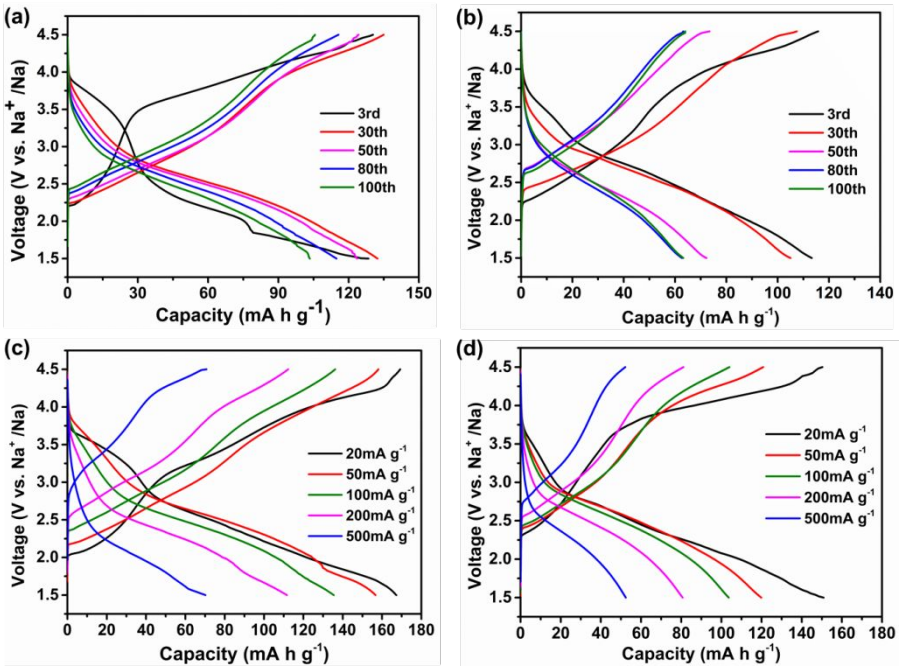


**Figure S5.** (a) The selected charge and discharge curves for s-NaLiMMCO at a rate of 100 mA $g^{-1}$. (b) The selected charge and discharge curves for i-NaLiMMCO at a rate of 100 mA $g^{-1}$. (c) Charge and discharge profiles at different rates for s-NaLiMMCO. (d) Charge and discharge profiles at different rates for i-NaLiMMCO.

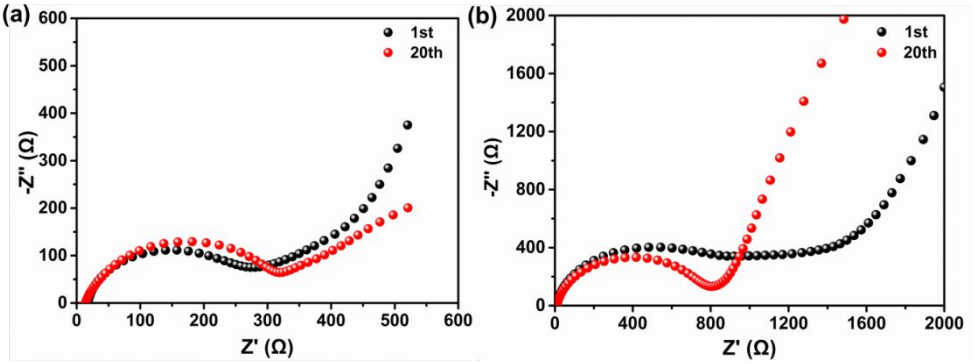


**Figure S6.** (a) The EIS spectra of the s-NaLiMMCO material for selected cycles at a rate of 20 mA $g^{-1}$. (b) The EIS spectra of the i-NaLiMMCO material for selected cycles at a rate of 20 mA $g^{-1}$.

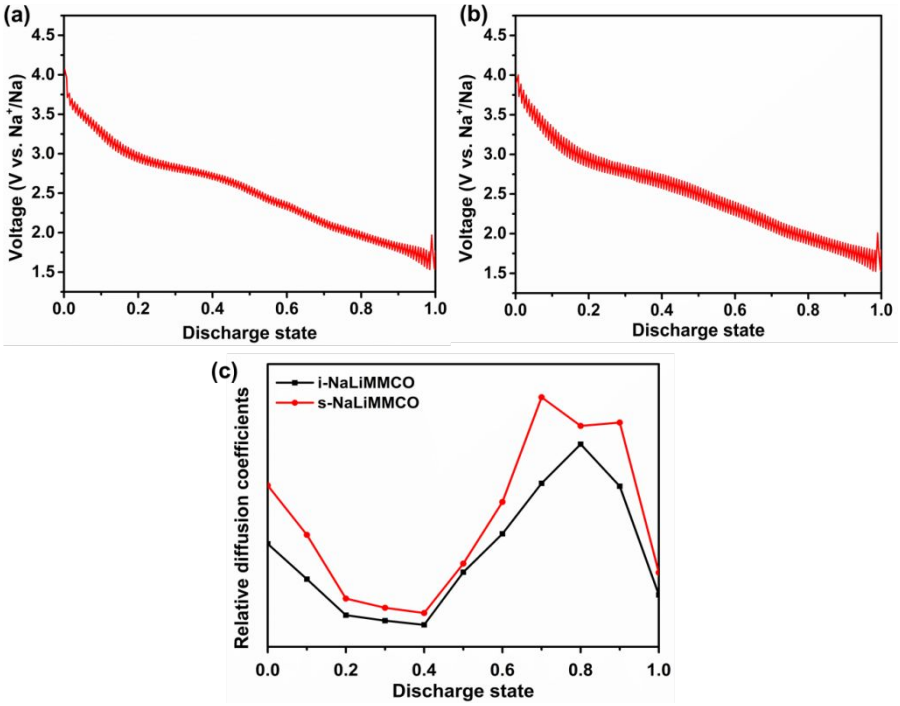


**Figure S7.** (a) GITT curves of s-NaLiMMCO. (b) GITT curves of i-NaLiMMCO. (c) The calculated Na chemical diffusion coefficients calculated from GITT measurement.

**Table S1.** ICP-OES results of solvothermal precursor

| Theoretical chemical formula | Measured atomic ratio | | |
|---|---|---|---|
| | Mn | Mg | Co |
| $Mn_{0.71}Mg_{0.21}Co_{0.08}CO_3$ | 0.71 | 0.20 | 0.08 |

**Table S2.** ICP-OES results of P2-$Na_{0.66}Li_{0.18}Mn_{0.71}Mg_{0.21}Co_{0.08}O_2$

| Theoretical chemical formula | Measured atomic ratio | | | | |
|---|---|---|---|---|---|
| | Na | Li | Mn | Mg | Co |
| $Na_{0.66}Li_{0.18}Mn_{0.71}Mg_{0.21}Co_{0.08}O_2$ | 0.65 | 0.18 | 0.69 | 0.20 | 0.07 |

**Table S3.** Electrochemical performance comparison for P2-type Mn-based cathode material.

| Cathode materials | Voltage range | Initial capacity (mA h $g^{-1}$) | Capacity retention | Ref. |
|---|---|---|---|---|
| $Na_{0.66}Li_{0.18}Mn_{0.71}Mg_{0.21}Co_{0.08}O_2$ | 1.5-4.5V | 166/20 mA $g^{-1}$ | 82% (100 cycle) | This work |
| $Na_{0.78}Ni_{0.23}Mn_{0.69}O_2$ | 2.0-4.5V | 138/0.1C | 90% (20 cycle) | 1 |
| $Na_{2/3}Fe_{1/2}Mn_{1/2}O_2$ | 1.5-4.3V | 126/13 mA $g^{-1}$ | 83% (30 cycle) | 2 |
| $Na_{0.67}Ni_{0.29}Co_{0.13}Mn_{0.58}O_2$ | 2.0-4.3V | 164.2/16 mA $g^{-1}$ | 77.4% (100 cycle) | 3 |
| $Na_{2/3}Ni_{1/3}Mn_{5/9}Al_{1/9}O_2$ | 1.6-4.0V | 118/0.1C | 77.5% (100 cycle) | 4 |
| $Na_{0.7}[Cu_xFe_yMn_{1-x-y}]O_2$ | 2.5–4.2V | 97.8/0.1C | 82% (80 cycle) | 5 |
| $Na_{2/3}Fe_{1/2}Mn_{1/2}O_2$ | 1.5–4.2V | 180 / 0.1C | 55% (80 cycle) | 6 |
| $Na_{0.66}Co_xMn_{0.66-x}Ti_{0.34}O_2$ | 2.0-4.3V | 130/0.2C | 81% (100 cycle) | 7 |
| $Na_{0.5}[Ni_{0.23}Fe_{0.13}Mn_{0.63}]O_2$ | 1.5-4.6V | 200/15 mA $g^{-1}$ | 75% (70 cycle) | 8 |
| $Na_{0.67}Mn_{0.65}Ni_{0.2}Co_{0.15}O_2$ | 1.5-4.2V | 155/12 mA $g^{-1}$ | 85% (100 cycle) | 9 |
| $Na_{0.67}Mn_{0.65}Fe_{0.2}Ni_{0.15}O_2$ | 1.5-4.5V | 204/0.05C | 71% (50 cycle) | 10 |
| $Na_{2/3}Ni_{1/3-x}Mg_xMn_{2/3}O_2$ | 2.0-4.5V | 150/10 mA $g^{-1}$ | 84% (50 cycle) | 11 |
| $Na_{2/3}(Mn_{1/2}Fe_{1/4}Co_{1/4})O_2$ | 1.5-4.5V | 195/0.1C | 71% (30 cycle) | 12 |
| $Na_{0.67}Mn_{0.67}Ni_{0.33-x}Mg_xO_2$ | 2.5-4.35V | 123/17 mA $g^{-1}$ | 85% (50 cycle) | 13 |
| $Na_{0.66}Ni_{0.26}Zn_{0.07}Mn_{0.67}O_2$ | 2.0-4.4V | 132/12 mA $g^{-1}$ | 89% (30 cycle) | 14 |
| $Na_{0.67}Ni_{0.2}Cu_{0.1}Mn_{0.7}O_2$ | 2.0-4.5V | 125.3/17 mA $g^{-1}$ | 72% (100 cycle) | 15 |
| $Na_{0.44}Mn_{0.6}Ni_{0.4-x}Cu_xO_2$ | 1.5-4.0V | 149.2/17 mA $g^{-1}$ | 80% (50 cycle) | 16 |
| $Na_{0.67}Mn_{0.8}Ni_{0.1}Mg_{0.1}O_2$ | 1.5-4.2V | 171/0.05C | 79% (50 cycle) | 17 |
| $Na_{0.67}Li_{0.2}(Ni_{0.2}Fe_{0.15}Mn_{0.65})_{0.8}O_2$ | 1.5-4.3V | 151/0.1C | 78% (50 cycle) | 18 |

**References**

(1) Ma, C.; Alvarado, J.; Xu, J.; Clement, R. J.; Kodur, M.; Tong, W.; Grey, C. P.; Meng, Y. S. Exploring oxygen activity in the high energy P2-type $Na_{0.78}Ni_{0.23}Mn_{0.69}O_2$ cathode material for Na-ion batteries. *J. Am. Chem. Soc.* **2017**, *139*, 4835-4845.

(2) Bai, Y.; Zhao, L.; Wu, C.; Li, H.; Li, Y.; Wu, F. Enhanced sodium ion storage behavior of P2-type $Na_{2/3}Fe_{1/2}Mn_{1/2}O_2$ synthesized via a chelating agent assisted route. *ACS Appl. Mater. Interfaces* **2016**, *8*, 2857-2865.

(3) Hou, P.; Li, F.; Wang, Y.; Yin, J.; Xu, X. Mitigating the P2–O2 phase transition of high-voltage P2-$Na_{2/3}[Ni_{1/3}Mn_{2/3}]O_2$ cathodes by cobalt gradient substitution for high-rate sodium-ion batteries. *J. Mater. Chem. A* **2019**, *7*, 4705-4713.

(4) Zhang, X. H.; Pang, W. L.; Wan, F.; Guo, J. Z.; Lu, H. Y.; Li, J. Y.; Xing, Y. M.; Zhang, J. P.; Wu, X. L. P2-$Na_{2/3}Ni_{1/3}Mn_{5/9}Al_{1/9}O_2$ microparticles as superior cathode material for sodium-ion batteries: enhanced properties and mechanisam via graphene connection. *ACS Appl. Mater. Interfaces* **2016**, *8*, 20650-20659.

(5) Xu, S.; Wu, J.; Hu, E.; Li, Q.; Zhang, J.; Wang, Y.; Stavitski, E.; Jiang, L.; Rong, X.; Yu, X.; Yang, W.; Yang, X.-Q.; Chen, L.; Hu, Y.-S. Suppressing the voltage decay of low-cost P2-type iron-based cathode materials for sodium-ion batteries. *J. Mater. Chem. A* **2018**, *6*, 20795-20803.

(6) Pang, W. K.; Kalluri, S.; Peterson, V. K.; Sharma, N.; Kimpton, J.; Johannessen, B.; Liu, H. K.; Dou, S. X.; Guo, Z. Interplay between electrochemistry and phase evolution of the P2-type $Na_x(Fe_{1/2}Mn_{1/2})O_2$ cathode for use in sodium-ion batteries. *Chem. Mater.* **2015**, *27*, 3150-3158.

(7) Wang, Q. C.; Hu, E.; Pan, Y.; Xiao, N.; Hong, F.; Fu, Z. W.; Wu, X. J.; Bak, S. M.; Yang, X. Q.; Zhou, Y. N., Utilizing $Co^{2+}/Co^{3+}$ redox couple in P2-layered $Na_{0.66}Co_{0.22}Mn_{0.44}Ti_{0.34}O_2$ cathode for sodium-ion batteries. *Adv. Sci.* **2017**, *4*, 1700219.

(8) Hasa, I.; Buchholz, D.; Passerini, S.; Scrosati, B.; Hassoun, J. High performance $Na_{0.5}[Ni_{0.23}Fe_{0.13}Mn_{0.63}]O_2$ cathode for sodium-ion batteries. *Adv. Energy Mater.* **2014**, *4*, 1400083.

(9) Li, Z.-Y.; Gao, R.; Sun, L.; Hu, Z.; Liu, X. Designing an advanced P2-$Na_{0.67}Mn_{0.65}Ni_{0.2}Co_{0.15}O_2$ layered cathode material for Na-ion batteries. *J. Mater. Chem. A* **2015**, *3*, 16272-16278.

(10) Yuan, D.; Hu, X.; Qian, J.; Pei, F.; Wu, F.; Mao, R.; Ai, X.; Yang, H.; Cao, Y. P2-type $Na_{0.67}Mn_{0.65}Fe_{0.2}Ni_{0.15}O_2$ cathode material with high-capacity for sodium-ion battery. *Electrochim.*

*Acta* **2014**, *116*, 300-305.

(11) Tapia-Ruiz, N.; Dose, W. M.; Sharma, N.; Chen, H.; Heath, J.; Somerville, J. W.; Maitra, U.; Islam, M. S.; Bruce, P. G. High voltage structural evolution and enhanced Na-ion diffusion in P2-$Na_{2/3}Ni_{1/3-x}Mg_xMn_{2/3}O_2$ ($0 \leq x \leq 0.2$) cathodes from diffraction, electrochemical and ab initio studies. *Energy Environ. Sci.* **2018**, *11*, 1470-1479.

(12) Liu, L.; Li, X.; Bo, S.-H.; Wang, Y.; Chen, H.; Twu, N.; Wu, D.; Ceder, G. High-performance P2-type $Na_{2/3}(Mn_{1/2}Fe_{1/4}Co_{1/4})O_2$ cathode material with superior rate capability for Na-ion batteries. *Adv. Energy Mater.* **2015**, *5*, 1500944.

(13) Wang, P. F.; You, Y.; Yin, Y. X.; Wang, Y. S.; Wan, L. J.; Gu, L.; Guo, Y. G. Suppressing the P2-O2 phase transition of $Na_{0.67}Mn_{0.67}Ni_{0.33}O_2$ by magnesium substitution for improved sodium-ion batteries. *Angew. Chem., Int. Ed.* **2016**, *55*, 7445-7449.

(14) Wu, X.; Guo, J.; Wang, D.; Zhong, G.; McDonald, M. J.; Yang, Y. P2-type $Na_{0.66}Ni_{0.33-x}Zn_xMn_{0.67}O_2$ as new high-voltage cathode materials for sodium-ion batteries. *J. Power Sources* **2015**, *281*, 18-26.

(15) Wang, L.; Sun, Y.-G.; Hu, L.-L.; Piao, J.-Y.; Guo, J.; Manthiram, A.; Ma, J.; Cao, A.-M. Copper-substituted $Na_{0.67}Ni_{0.3-x}Cu_xMn_{0.7}O_2$ cathode materials for sodium-ion batteries with suppressed P2–O2 phase transition. *J. Mater. Chem. A* **2017**, *5*, 8752-8761.

(16) Chen, T.; Liu, W.; Gao, H.; Zhuo, Y.; Hu, H.; Chen, A.; Zhang, J.; Yan, J.; Liu, K. A P2-type $Na_{0.44}Mn_{0.6}Ni_{0.3}Cu_{0.1}O_2$ cathode material with high energy density for sodium-ion batteries. *J. Mater. Chem. A* **2018**, *6*, 12582-12588.

(17) Li, Z.-Y.; Gao, R.; Zhang, J.; Zhang, X.; Hu, Z.; Liu, X. New insights into designing high-rate performance cathode materials for sodium ion batteries by enlarging the slab-spacing of the Na-ion diffusion layer. *J. Mater. Chem. A* **2016**, *4*, 3453-3461.

(18) Wang, Y.; Hu, G.; Peng, Z.; Cao, Y.; Lai, X.; Qi, X.; Gan, Z.; Li, W.; Luo, Z.; Du, K. Influence of Li substitution on the structure and electrochemical performance of P2-type $Na_{0.67}Ni_{0.2}Fe_{0.15}Mn_{0.65}O_2$ cathode materials for sodium ion batteries. *J. Power Sources* **2018**, *396*, 639-647.